https://doi.org/10.18321/ectj997

PCL Based CIP-Loaded Double-Layer Films Deposited by Low-Electron Beam Dispersion Method and its Antibacterial Properties

Qin Xu[1], Beibei Li[1], Zhengwei Xu[1], Xiaohong Jiang[1]*, M.A. Yarmolenko[2], A.A. Rogachev[2], A.V. Rogachev[2]

[1]International Chinese-Belorussian Scientific Laboratory on Vacuum-Plasma Technology, Nanjing University of Science and Technology, 200, Xiaolingwei str., Nanjing 210094, China
[2]Francisk Skorina Gomel State University, 104, Sovetskaya str., Gomel 246019, Belarus

Article info

Received:
9 February 2020

Received in revised form:
18 April 2020

Accepted:
28 May 2020

Keywords:
Low-electron beam dispersion
Polycaprolactone
Polyurethane
Ciprofloxacin
Antibacterial activity
Drug release

Abstract

In this paper, low-electron beam dispersion (EBD) method is used to prepare a kind of double-layer films on different substrates. The bottom layer is a mechanically stirred mixture of the degradable polycaprolactone (PCL) and ciprofloxacin (CIP), and the top layer is polyurethane (PU) film. The molecular structure, chemical composition and morphology of the double-layer films were investigated by FTIR, XPS and SEM. The results showed that the surfaces of the double-layer films are uniform and the thicknesses can reach micron level. In addition, the two layers are well bonded. Then the films were sliced and immersed in PBS solution, and the time-dependent variable was used to analyze the kinetic slow-release behavior of CIP in the double-layer films by agar diffusion antibacterial experiments. It can be seen that sustained release time of CIP in the double-layer films can be up to 7 days, which is due to fact that the upper PU film working as a sealing layer helps to realize the drug slow-release. Based on the above research, the comprehensive performance of the films with the composition of PCL:CIP/PU=1:1/1 is the best.

1. Introduction

Nowadays, most artificial implants used in hospitals are facing various problems such as inflammation, rejection, allergic reactions and biofilms produced from varying degrees of pathogen adhesion [1]. With the purpose of ensuring that implant materials like hip and knee joints can continuously and stably work in the human environment, it is essential to achieve biofilm inhibition and reduce bacterial infections. In this paper, we are committed to depositing biodegradable drug-loaded polymer films on titanium (Ti) substrates to regulate drug delivery and endow long-term antibacterial properties [2–3]. Ciprofloxacin, whose antibacterial ability is proved to be 2–4 times that of norfloxacin and enoxacin [4], is an effective broad-spectrum antibiotic applied in the medical industry now. What's more, Ciprofloxacin can restrain the colonization of multiple bacterium, such as *Escherichia coli*, *Pseudomonas aeruginosa*, *Haemophilus influenzae*, *Neisseria gonorrhoeae*, *Streptococcus*, *Legionella* and *Staphylococcus aureus* [5].

In the past ten years, synthetic polyester PCL has received special attention. Poly-ε-caprolactone (PCL) is a biodegradable and biocompatible semi-crystalline polymer with a low glass transition temperature (-60 °C) [6]. When in the human's body, the cells can grow normally on their base frame and can be degraded into CO_2 and H_2O. In addition, it also can be well compatible with polyethylene (PE), polypropylene (PP), styrene resin (ABS), polyurethane (PU), natural rubber, etc. [7–9]. PU is a nontoxic polymer with prominent biocompatibility, biodegradation, antibacterial ability and mechanical properties including wear resistance and easy processing, which possesses promising application prospect in a variety of biomedical fields especially controlled drug release [10].

*Corresponding author.
E-mail: jiangxh24@njust.edu.cn

According to the above-mentioned, we expect to construct biodegradable films by low-electron beam dispersion and CIP machinery mixed with PCL or coated by PU is chosen as the target materials for the deposition. Since the nature of the polymers used, target composition and laser intensity generated by the deposition device will probably affect the structure and performance of the films required, regulation of relevant influence factors can help to achieve the optimum preparation processing by evaluation of bioactivity and cytotoxicity.

Nowadays, the most widely used preparation methods are mainly divided into physical vapor deposition (PVD) and chemical vapor deposition (CVD). EBD is a PVD method carrying out rapid deposition and simple operation and the dispersion of electron beam is beneficial to obtain uniform high-purity and high-density films [11]. Vacuum evaporation is conducive to avoid the contamination and oxidation of the target materials and form an antibacterial layer which can prolong the drug release time [12].

2. Materials and methods

2.1. Methodology of forming coatings

EBD is one of the vapor deposition methods. A low-energy electron beam of 800–1600 eV and 0.01–0.03 A/cm^2 was used to excite the target to a highly active state with the purpose of deposition on Ti substrates. This whole process was performed in a high vacuum (5×10^{-4} Pa) and the chamber temperature was close to the room temperature which is normally about 25 °C.

2.2. Materials and preparation of double-layer films

In this article, we choose polycaprolactone (PCL, Mw~5000) powder, ciprofloxacin hydrochloride (CIP) powder and polyurethane (PU, Desmopan 385) as target materials to deposit the double-layer films. In addition, the substrate is made of titanium (Ti) with 0.1 mm thickness (microbiological analysis, XPS), silicon (Si) (SEM analysis) and KBr plates (FTIR analysis).

The ultrasonic cleaning of Ti sheets with 0.1 mm thickness was performed in deionized water and alcohol for 15 min each, cycling three times. For the first layer deposition, targets containing PCL and ciprofloxacin (1:1, mass ratio), whose composition was based on our previous research, were used [13]. PU was deposited on the underlying layer and the mass ratios are PCL:CIP/PU=1:1/0.5, PCL:CIP/PU=1:1/1, PCL:CIP/PU=1:1/2 respectively).

2.3. Study on antibacterial and sustained release properties

The film-coated titanium sheet was cut into 6 mm diameter discs as a sample to study its antibacterial properties and drug release durability. Put the sample into 5 ml phosphate buffer saline (PBS) and keep the temperature at 36.6 °C for different times (1d, 3d, 7d). The next step was taking out the sample and solution separately. The soaked sample was used in the antibacterial experiment of the solid agar diffusion method.

As it was shown that the antibacterial activity of CIP was tested against *E. coli* ATCC 25922 and *S. aureus* ATCC 12600 using the agar diffusion method on the solid LB agar medium [11]. It had proved that CIP has stronger antibacterial activity against *S. aureus* than *E. coli*, so in this article, we choose *S. aureus* to test.

2.4. Structure and morphology studies

On one hand, the films were deposited on Ti sheets, and the surface structure and morphologies were observed from SEM images. On the other hand, the silicon wafers deposited with films of different compositions were quenched by liquid nitrogen, and then the cross-section morphologies were also investigated by SEM to conduct film thickness measurements.

3. Results and discussion

3.1. The results of FTIR spectroscopic analysis

As shown in Fig. 1/1, characteristic peaks of CIP powder are evident at 1702 cm^{-1} and 1616 cm^{-1}, corresponding to the stretching vibration of C=O of the carboxylic acid and the C=C stretching vibration in the quinoline ring [14]. While at 1270 cm^{-1}, the coupling of C-O stretching vibration in the carboxylic acid and the O-H deformation vibration is observed. The IR spectrum of PCL powder in Fig. 1/2 has its characteristic absorption peak of NHCOO- at 1725 cm^{-1} [15]. In Fig. 1/3, after mechanical mixing and EBD deposition, the IR spectrum of the single-layer film (PCL:CIP=1:1, mass ratio) is characterized by the presence of a broad absorption band at 1100–1300 cm^{-1} caused by the stretching vibration of C-O-C bond, which exists in both PCL and CIP [16]. Apart from this peak, the stretching vibration of carboxylic acid and ketone C=O stretching vibration is located at 1725 cm^{-1} and 1620 cm^{-1}, respectively. It confirms that PCL and CIP are integrated and are relatively

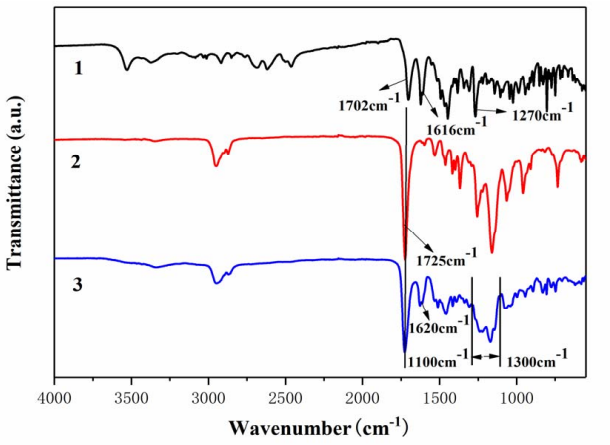

Fig. 1. FTIR spectra of films and powders: 1 – ciprofloxacin powders; 2 – PCL powders; 3 – PCL:CIP=1:1 film.

tightly and uniformly mechanically mixed together. These results indicate that the CIP powder did not degrade significantly under the activation of low-electron beams, which is attributed to the fact that the tendency of ciprofloxacin evaporation is accessible without strong heating and radiation exposure [11].

Figure 2/1 is the IR spectrum of PU powders. The most pronounced characteristic peak of PU is N-H vibration which forms at 3340 cm^{-1}. Besides, the peaks at 2864 cm^{-1} and 2952 cm^{-1} are attributed to symmetric and asymmetric stretching vibrations of CH_2 bond, respectively [17]. The moderate intensity peak located at 1528 cm^{-1} is the in-plane bending vibration of N-H bond [18]. However, with regard to the newly deposited double-layer films (PCL:CIP/PU=1:1/0.5) (Fig. 2/3), the relative intensity of the characteristic peak of the

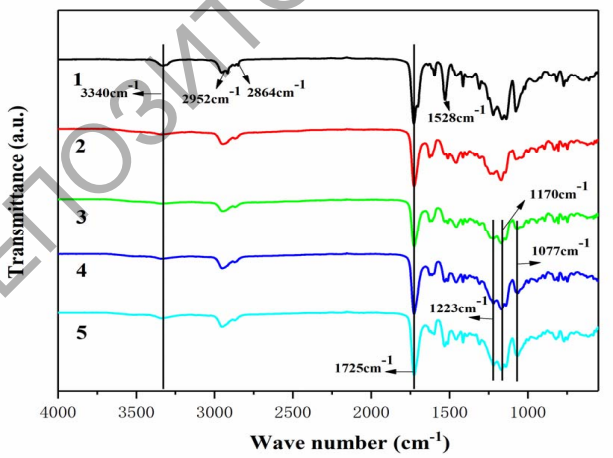

Fig. 2. FTIR spectra of films and powders 1 – PU powders; 2 – PCL:CIP=1:1 film; 3 – PCL:CIP/PU=1:1/0.5 films; 4 – PCL:CIP/PU=1:1/1 films; 5 – PCL:CIP/PU=1:1/2 films.

whole functional group is declined as the result of the characteristic peak at 1725 cm^{-1} is the carboxylic acid C=O shared by PCL, CIP and PU, which is more intense after mixing compared with original PU powders and the single-layer film (Fig. 2/2). With the PU content increasing (Fig. 2/3, 2/4, 2/5), the stretching vibration of C-O-C bond is located at 1223 cm^{-1}, 1170 cm^{-1}, 1077 cm^{-1} becomes stronger while the characteristic peak of N-H, which is detected at 3340 cm^{-1} and the stretching vibration of bond belonging to C=O at 1725 cm^{-1} gradually becomes prominent. This proves that the characteristic peaks of the functional groups of PCL, CIP and PU partly overlap and are integrated. This may be due to the reason that during the deposition of the film, hydrogen bonds (-H) are formed between different components, and the -H formed between different macromolecules is stronger than the -H formed between the same polymer. Non-phenanthrene behavior that can be described and explained using the adsorption mechanism also exists between PCL and PU, which makes the connection between the two layers of the films tight [19].

3.2. XPS analysis results

The chemical composition of the double-layer films consisting of C, O, N, and F elements are listed in Table 1. XPS spectroscopic analysis of the composite layer is difficult. This is mainly due to the non-stationary process of the dispersion of the composite target.

The chemical composition of the double-layer films is studied by decomposition of the C1s band into individual peaks (Fig. 3). The XPS analysis results show that the composite peak of C1s was decomposed into composite peaks centered at 284.8 eV (corresponding to the C-C bond in PCL, CIP, PU), and the other two peaks are located at 288.7 eV (C=O, C=C, C–F) and 286.17 eV (C-O, C-N) [20, 21]. The peak areas account for 58.1%, 31.6%, and 10.3%, respectively.

Table 1
The results of the elemental compositions of the films

Films	Atomic percentage (%)			
	C	O	N	F
PCL:CIP=1:1	71.5	21.6	5.4	1.5
PCL:CIP/PU=1:1/0.5	72.4	25.7	1.4	0.5
PCL:CIP/PU=1:1/1	74.6	23.2	2.1	<0.1
PCL:CIP/PU=1:1/2	71.6	27.5	0.9	<0.1

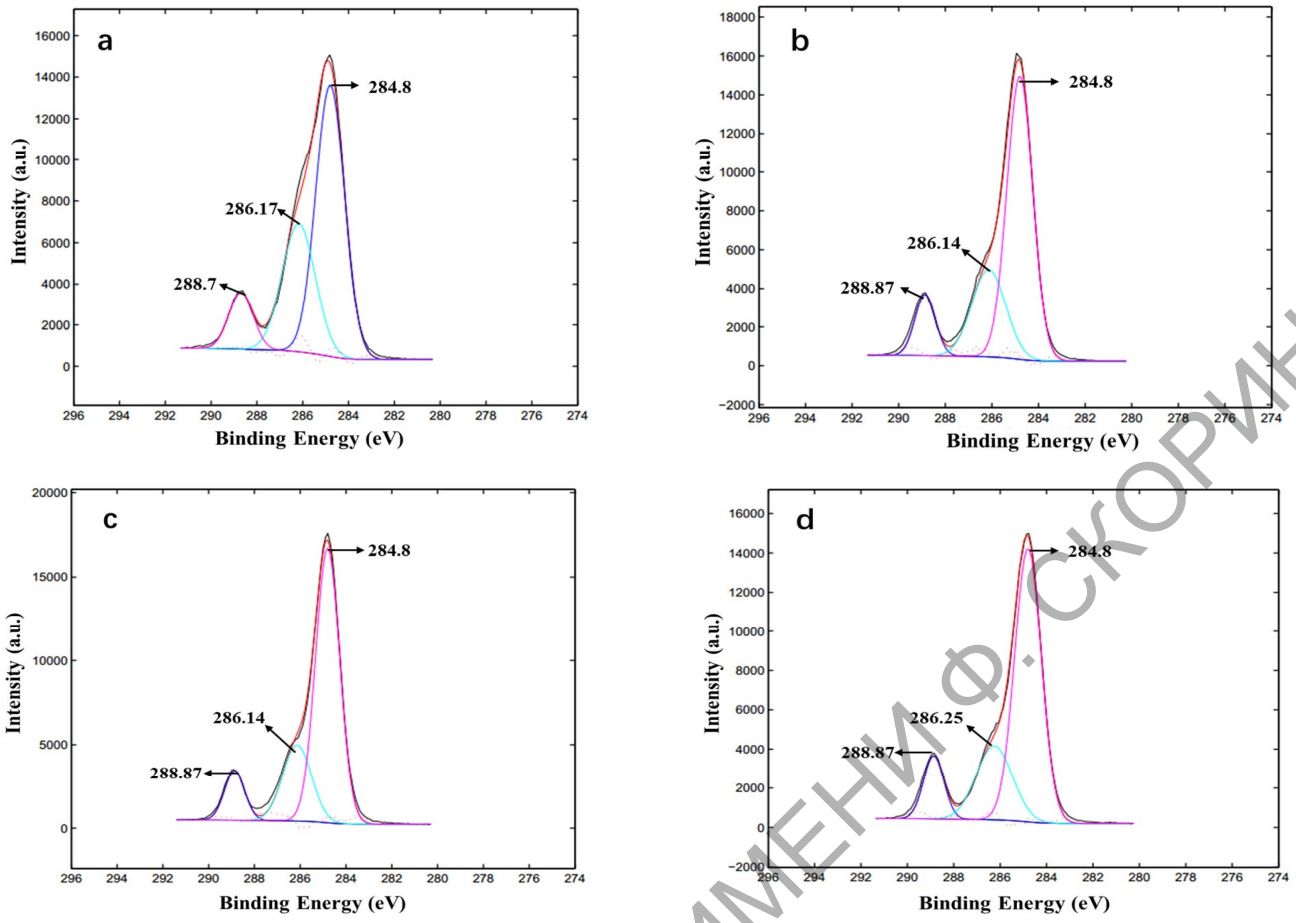

Fig. 3. XPS spectra of C1s: a – PCL:CIP=1:1 film; b – PCL:CIP/PU=1:1/0.5 films; c – PCL:CIP/PU=1:1/1 films; d – PCL:CIP/PU=1:1/2 films.

Compared with the single-layer film, the peak height of the central peak C-C and the area fraction of the peak have a high growth in the double-layer films (the average value is about 65.4%). This is because the higher the content of PU, the larger the proportion of C-C in the total carbon-containing chemical bonds. Meanwhile, the peaks characterized as C=O, C=C and C–F bonds shift to higher binding energy positions and are located at 288.87 eV, which indicates the variation of chemical states. Besides, the height of the peak (C-O, C-N) decreases from 11263 to 7567 (average of double-layer films of different PU contents). It indicates there is a decrease in the content of nitrogen atoms as a result of an intense degradation process of both components which interact with each other tightly in the influence zone of the electron beam [22].

In addition, there is only one peak related to F1s centering at 684.95 eV, and the peak height (1239, 235, 172, 0) continuously decreases with PU mass ratio increasing (Fig. 4). As fluorine is an element that exists only in CIP of the double-layer films, after PU wraps the bottom film, fluorine is also supposed to be coated by PU. It should be noted that XPS can only excite electrons on the surface without energy loss, so the range of the element can only be accurately measured within 10 nm of the surface thickness [23]. Therefore, the higher the thickness of the upper layer PU, the less fluorine atomic content detected.

In conclusion, the characteristic functional groups of CIP in the double-layer composite films still exist, which is consistent with the FTIR analysis.

3.3. The results of morphological analysis

Figure 5 shows the surface morphology of the single-layer film (PCL:CIP=1:1) (Fig. 5A) and the double-layer films (PCL:CIP/PU=1:1/1) (Fig. 5B). It can be seen that the surface of the single-layer film is lotus shaped with a few folds, which is basically uniform and flat. It is a significant morphological transformation can be observed while there are many cracks on the CIP film [13]. Compared with the single-layer film, there are many hemispherical protrusions of different sizes (1–30 μm),

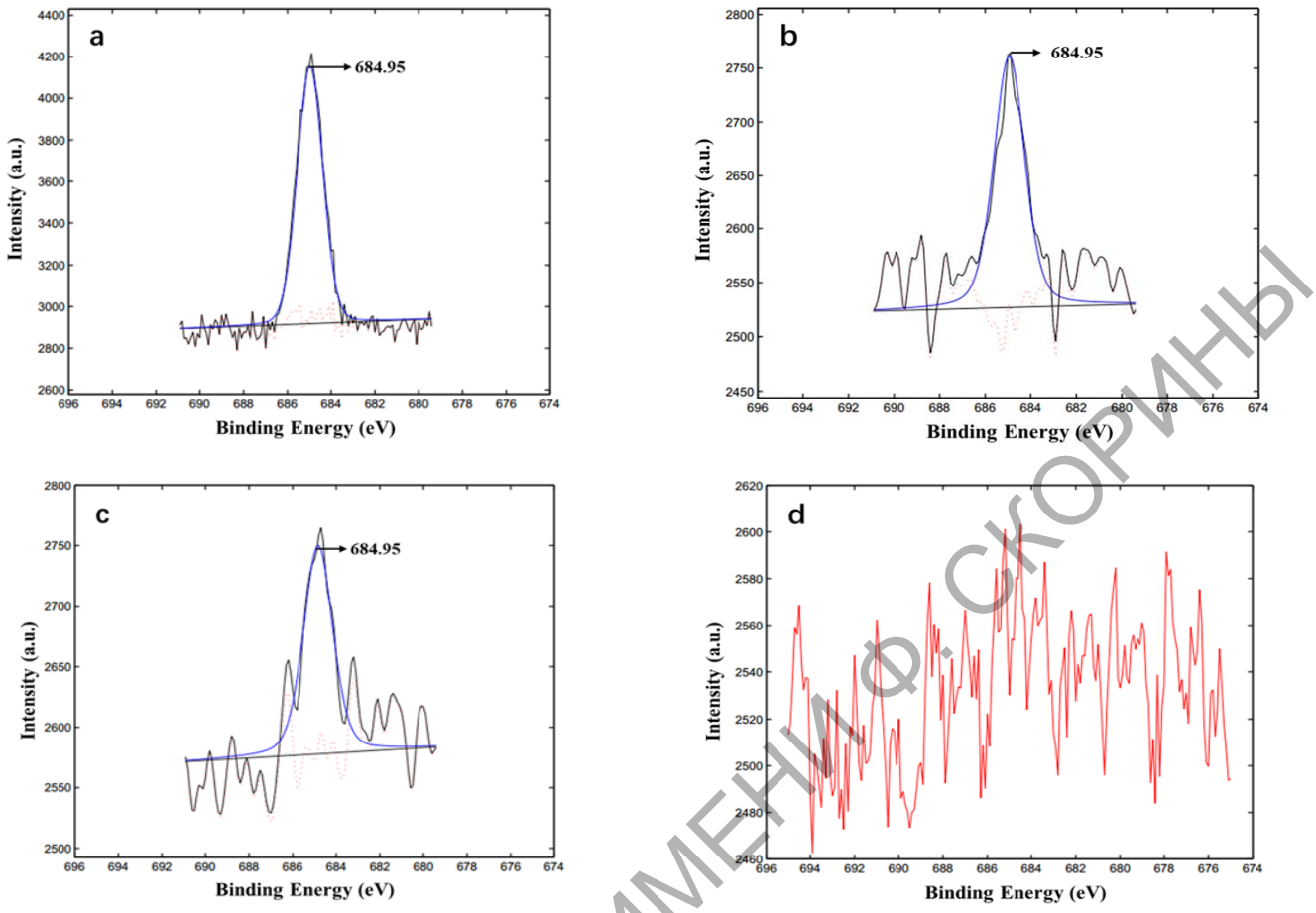

Fig. 4. XPS spectra of F1s: a – PCL:CIP=1:1 film; b – PCL:CIP/PU=1:1/0.5 films; c – PCL:CIP/PU=1:1/1 films; d – PCL:CIP/PU=1:1/2 films

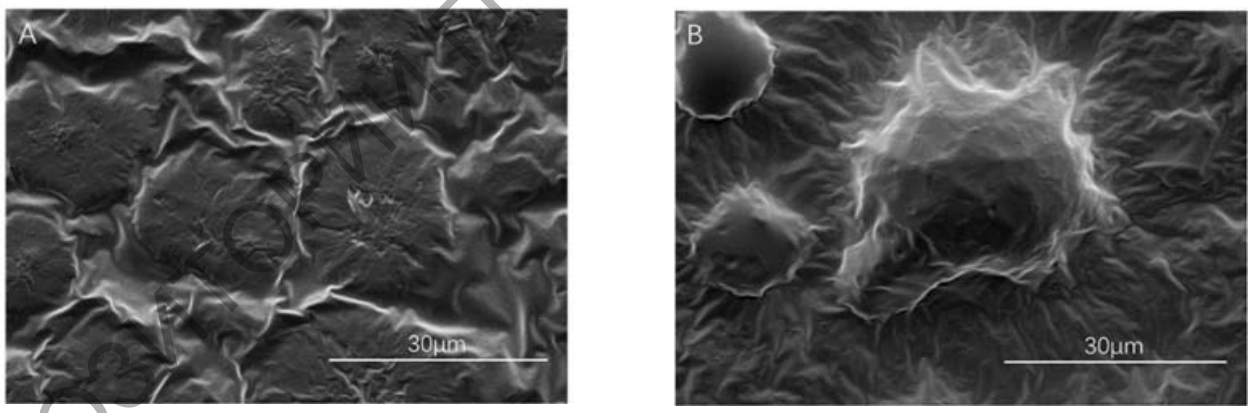

Fig. 5. SEM images of the surface morphologies of different composite layers A-PCL:CIP=1:1 film; B-PCL:CIP/PU=1:1/1films.

which indicates the existence of PU, on the surface of the double-layer films. In addition, the mountain-shaped bulges on the surface are obtained, which may be explained by the unevenness of the film during the deposition process as the film thickness increases.

The cross-sectional images of the film thickness are displayed in Fig. 6. The film thicknesses are diverse from each other but they are all in micron scale. The single-layer film (PCL:CIP=1:1) has a film thickness of 1.76 μm, and the double-layer films have film thicknesses of 2.23 μm (PCL:CIP/PU=1:1/0.5), 3.5 μm (PCL:CIP/PU=1:1/1), and 4.26 μm (PCL:CIP/PU=1:1/2) related to the PU content. In conclusion, with the increase of PU content, the growth rate of the film is 26.7%, 57% and 21.7% respectively. It can be found that the film grows sharpest when the ratio of PU increases

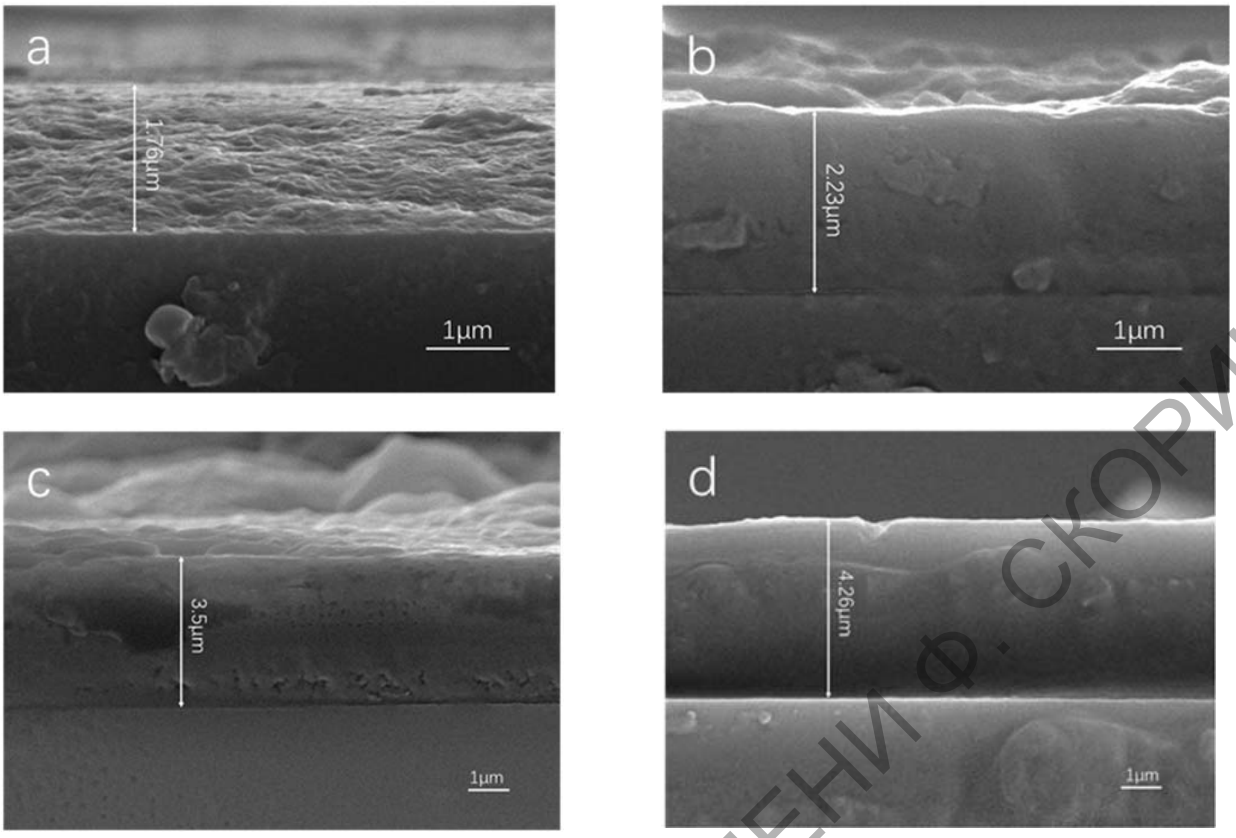

Fig. 6. SEM cross-sectional images of different composite layers: a – PCL:CIP=1:1 film; b – PCL:CIP/PU=1:1/0.5 films; c – PCL:CIP/PU=1:1/1 films; d – PCL:CIP/PU=1:1/2 films.

from 0.5 to 1. This may be due to the amount of PU are few when the mass ratio of PCL:CIP/PU=1:1/0.5, and the bonding with the underlying film is not tight enough, which leads to some PU powder cannot be deposited totally. However, for the sample with the mass ratio of PCL:CIP/PU=1:1/2, as a result of the long deposition time, the PU loss during the deposition process also increases. It needs to be pointed out that when the mass ratio is PCL:CIP/PU=1:1/1, the highest PU utilization rate and the best deposition quality attract our attention.

3.4. The results of the antibacterial analysis

As is shown in Fig. 7 of the initial microbial inhibition area (0d), the composite films are obviously resistant to *S. aureus* and have good antibacterial performance. Ciprofloxacin is a broad-spectrum antibiotic with a selective inhibitory effect on bacterial DNA helicase, weakening the function of DNA helicase from the active DNA-gyrase binding site (3-oxo-4-carboxylic acid core) [24, 25]. This can be summarized that ciprofloxacin exhibits its broad-spectrum activity against Gram-negative and Gram-positive bacteria by inhibiting bacterial DNA replication, which leads to bacterial reproductive disorder and death.

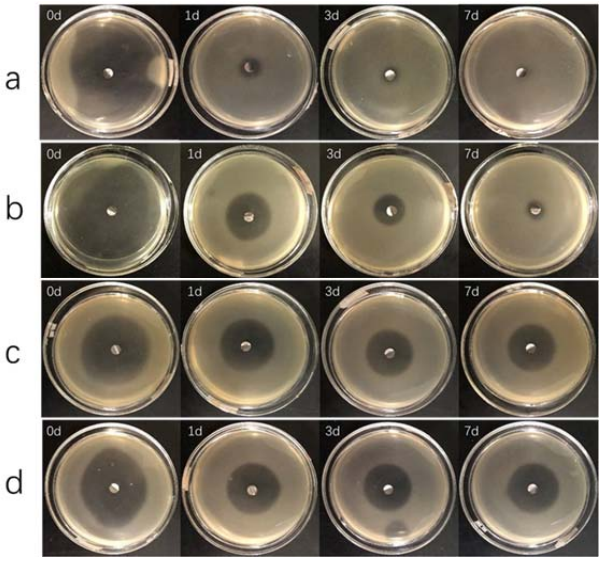

Fig. 7. The images of change in the diameter of the inhibition zone of *S. aureus* growth by the different composite layers with release times: a – PCL:CIP=1:1 film; b – PCL:CIP/PU=1:1/0.5 films; c – PCL:CIP/PU=1:1/1 films; d – PCL:CIP/PU=1:1/2 films

Table 2
The numbers of the inhibition zone (D/mm) of *S. aureus* growth by the different composite layers with release times change in the diameter

PCL:CIP/PU (mass ratio)	Release time			
	0d	1d	3d	7d
1:1/0	60	13	8	0
1:1/0.5	70	28	20	11
1:1/1	45	31	29	30
1:1/2	46	32	30	31

The study on the change of the antibacterial activity of the double-layer films during their exposure in the PBS solution is carried out (Fig. 7). According to the antibacterial experiment, the inhibition zones around the films without immersion in PBS solution for drug release are the largest. The diameter of the inhibition zone of *S. aureus* decreases monotonously with an increase in the coating duration of immersion in the PBS solution. In the process of immersion in the PBS solution, CIP in direct contact with the solution is released gradually and the degradation of PCL is conducive to the controlled drug release. Besides, the boundary blurring of the antibacterial circle is observed. It is most obviously appeared in the single-layer film without PU where the diameter of the inhibition zone was 0 mm after 7 days which indicates the bacteriostatic activity of the film completely disappeared.

In contrast, the double-layer films containing PU retained antibacterial activity after 7 days of soaking, and with the increase of immersion time, the diameter of the inhibition circle shrinks at different rates with the decrease of PU content. For the sample with the film composition of PCL:CIP/PU=1:1/0.5, the diameter of the inhibition circle decreases most obviously in the whole immersing process and the reduction rate is separated from the condition of other PU-doped films, which still exhibit antibacterial activity, that inhibition circles have no significant change. This is primarily due to the second film PU who covers the surface of the single-layer film that plays an important role in slowing down the degradation of PCL. Therefore, the PBS solution must swell the PU initially to create holes before it reaches the bottom composite film. In conclusion, the relatively better antibacterial activity and sustained release performance have been achieved in the sample with the film composition of PCL:CIP/PU=1:1/1, and there is no need to further increase the thickness of PU.

4. Conclusion

In summary, from FTIR and XPS analysis, it is confirmed that PCL:CIP single-layer film and PCL:CIP/PU double-layer films were successfully prepared on substrates by EBD method. For the single-layer film, CIP is relatively evenly distributed in PCL. The composite material of PCL and CIP can be regarded as a highly dispersed mechanical mixture of the initial compounds, while chemical bonds have not been established between components with different natures. For the double-layer films, the EBD method successfully deposits samples with different PU contents, and hydrogen bonds have been formed between macromolecules with the bottom composite layer, establishing a tight connection between two layers. Besides, it can be seen from the SEM images that both single-layer film and double-layer films are continuous as the result of no significant micro-cracks on the surfaces which indicates that materials are deposited uniformly on the substrate. As the proportion of PU increases, the films also become thicker, while the growth rates increase first and then decrease. The values are 26.7%, 57% and 21.7%. Finally, as for the investigation of antibacterial properties and drug release performance, it should be noted that the double-layer films are obviously better than the single-layer in this respect. The samples with film compositions of PCL:CIP/PU=1:1/1 and PCL:CIP/PU=1:1/2 have better performances and the retention rates of their inhibition circles are 33.3% and 32.6% respectively after 7 days of continuous drug release. Stated thus, the double-layer films with the composition of PCL:CIP/PU=1:1/1 have the best antibacterial activity, sustained drug release performance and the highest material utilization rate among the samples.

Acknowledgement

This work was supported by the Intergovernmental Cooperation Projects in the National Key Research and Development Plan of the Ministry of Science and Technology of the People's Republic of China (No. 2016YFE0111800), and Nanjing University of Science & Technology Independent Research Project (No. 30919013301).

References

[1]. Y.-K. Wu, N.-C. Cheng, C.-M. Cheng, *Trends Biotechnol.* 37 (2019) 505–517. DOI: 10.1016/j.tibtech.2018.10.011

[2]. A.J.T. Teo, A. Mishra, I. Park, Y.-J. Kim, W.-T. Park, Y.-J. Yoon, *ACS Biomater. Sci. Eng.* 2 (2016) 454–472. DOI: 10.1021/acsbiomaterials.5b00429

[3]. H.O. Gbejuade, A.M. Lovering, J.C. Webb, *Acta Orthop.* 86 (2015) 147–158. DOI: 10.3109/17453674.2014.966290

[4]. S.A. Al-Trawneh, J.A. Zahra, M.R. Kamal, M.M.El-Abadelah, F. Zani, M. Incerti, A. Cavazzoni,R.R. Alferi, P.G. Petronini, P. Vicini, *Bioorg. Med. Chem.* 18 (2016) 5873–5884. DOI: 10.1016/j.bmc.2010.06.098

[5]. P.K. Dutta, S. Tripathi, G.K. Mehrotra, J. Dutta, *Food Chem.* 114 (2009) 1173–1182. DOI: 10.1016/j.foodchem.2008.11.047

[6]. M. Labet, W. Thielemans, *Chem. Soc. Rev.* 38 (2009) 3484–3504. DOI: 10.1039/b820162p

[7]. H.Y. Kweon, M.K. Yoo, I.K. Park, T.H. Kim, H.C. Lee, H.-S. Lee, J.-S. Oh, T. Akaike, C.-S. Cho, *Biomaterials* 24 (2003) 801–808. DOI: 10.1016/s0142-9612(02)00370-8

[8]. L. Averous, L. Moro, P. Dole, C. Fringant, *Polymer* 41 (2000) 4157–4167. DOI: 10.1016/S0032-3861(99)00636-9

[9]. J.M. Williams, A. Adewunmi, R.M. Schek, C.L. Flanagan, P.H. Krebsbach, S.E. Feinberg, S.J. Hollister, S. Das, *Biomaterials* 26 (2005) 4817–4827. DOI: 10.1016/j.biomaterials.2004.11.057

[10]. J.M.H. Kuijpens, G.A. Kardaun, R. Blezer, A.P. Pijpers, L.H. Koole, *J. Am. Chem. Soc.* 117 (1995) 8691–8697. DOI: 10.1021/ja00139a001

[11]. B. Li, C. He, X. Jiang, M.A. Yarmolenko, D.G. Piliptsou, A.A. Rogachev, A.V. Rogachev, B. Du, *Eurasian Chem.-Technol. J.* 22 (2020) 35–42. DOI: 10.18321/ectj928

[12]. C. He, A.V. Rogacheva, B. Li, V.A. Yarmolenko, A.A. Rogacheva, D.V. Tapal'skii, X. Jiang, D. Sun, M.A. Yarmolenko, *Surf. Coat. Tech.* 354 (2018) 38–45. DOI: 10.1016/j.surfcoat.2018.09.013

[13]. L.I. Beibei, H.E Chun, J. Xiaohong, M.A. Yrmolenko, D.G. Piliptsou, A.A. Rogahev, *Journal of Nanjing Tech University* (Natural Science Edition) 42 (2020) 743–750 (in Chinese). DOI: 10.3969/ j.issn.1671-7627.2020.06.009

[14]. G. Ajmal, G.V. Bonde, P. Mittal, G. Khan, V.K. Pandey, B.V. Bakade, B. Mishra, *Int. J. Pharmaceut.* 567 (2019) 118480. DOI: 10.1016/j.ijpharm.2019.118480

[15]. B. Feng, T. Ji, X. Wang, W. Fu, L. Ye, H. Zhang, F. Li, *Mater. Design* 193 (2020) 108773. DOI: 10.1016/j.matdes.2020.108773

[16]. S. Mohandesnezhad, Y. Pilehvar-Soltanahmadi, E. Alizadeh, A. Goodarzi, S. Davaran, M. Khatamian, N. Zarghami, M. Samiei, M. Aghazadeh, A. Akbarzadeh, *Mater. Chem. Phys.* 5 (2020) 123152. DOI: 10.1016/j.matchemphys.2020.123152

[17]. P. Demir, F. Akman, *J. Mol. Struct.* 1134 (2017) 404–415. DOI: 10.1016/j.molstruc.2016.12.101

[18]. S. Xu, X. Li, G. Sui, R. Du, Q. Zhang, Q. Fu, *Chem. Eng. J.* 381 (2020) 122666. DOI: 10.1016/j.cej.2019.122666

[19]. M.A. Parker, D. Vesely, *J. Polym. Sci. Pol. Phys.* 24 (1986) 1869–1878. DOI: 10.1002/polb.1986.090240821

[20]. Y. Fei, Y. Li, S. Han, J. Ma, *J. Colloid Interf. Sci.* 484 (2016) 196–204. DOI: 10.1016/j.jcis.2016.08.068

[21]. S. Park, S. Jung, J. Heo, J. Hong, *J. Ind. Eng. Chem.* 77 (2019) 97–104. DOI: 10.1016/j.jiec.2019.04.023

[22]. B. Li, Y. Liu, A.V. Rogachev, V.A. Yarmolenko, A.A. Rogachev, A.E. Pyzh, X. Jiang, M.A. Yarmolenko, *Mat. Sci. Eng. C-Mater.* 110 (2020) 110730. DOI: 10.1016/j.msec.2020.110730

[23]. I.S. Zhidkov, E.Z. Kurmaev, S.O. Cholakh, E. Fazio, L. D'Urso, *Mendeleev Commun.* 30 (2020) 285–287. DOI: 10.1016/j.mencom.2020.05.007

[24]. C. Zhi, Z.-yu Long, A. Manikowski, J. Comstock, W.-C. Xu, N.C. Brown, P.M. Tarantino, K.A. Holm, E.J. Dix, G.E. Wright, M.H. Barnes, M.M. Butler, K.A. Foster, W.A. LaMarr, B. Bachand, R. Bethell, C. Cadilhac, S. Charron, S. Lamothe, I. Motorina, R. Storer, *J. Med. Chem.* 49 (2006) 1455–1465. DOI: 10.1021/jm0510023

[25]. X. Li, Y.-K. Zhang, J.J. Plattner, W. Mao, M.R.K. Alley, Yi Xia, V. Hernandez, Y. Zhou, C.Z. Ding, J. Li, Z. Shao, H. Zhang, M. Xu, *Bioorg. Med. Chem. Lett.* 23 (2013) 963–966. DOI: 10.1016/j.bmcl.2012.12.045fluoroquinolone